Structure-Based Design and Synthesis of Lipophilic 2,4-Diamino-6-Substituted Quinazolines and Their Evaluation as Inhibitors of Dihydrofolate Reductases and Potential Antitumor Agents[1]

Aleem Gangjee,*[,†] Anup P. Vidwans,[†] Anil Vasudevan,[†,⊥] Sherry F. Queener,[‡] Roy L. Kisliuk,[∥] Vivian Cody,[§] Ruming Li,[§] Nikolai Galitsky,[§] Joe R. Luft,[§] and Walter Pangborn[§]

Division of Medicinal Chemistry, Graduate School of Pharmaceutical Sciences, Duquesne University, Pittsburgh, Pennsylvania 15282, Department of Pharmacology and Toxicology, School of Medicine, Indiana University, Indianapolis, Indiana 46202, Department of Biochemistry, School of Medicine, Tufts University, Boston, Massachusetts 02111, and Hauptman-Woodward Medical Research Institute Inc., 73 High Street, Buffalo, New York 14203

Received February 5, 1998

The synthesis and biological activities of 14 6-substituted 2,4-diaminoquinazolines are reported. These compounds were designed to improve the cell penetration of a previously reported series of 2,4-diamino-6-substituted-pyrido[2,3-*d*]pyrimidines which had shown significant potency and remarkable selectivity for *Toxoplasma gondii* dihydrofolate reductase (DHFR), but had much lower inhibitory effects on the growth of *T. gondii* cells in culture. The target N9−H analogues were obtained via regiospecific reductive amination of the appropriate benzaldehydes with 2,4,6-triaminoquinazoline, which, in turn, was synthesized from 2,4-diamino-6-nitroquinazoline. The N9−CH_3 analogues were synthesized via a regiospecific reductive methylation of the corresponding N9−H precursors. The compounds were evaluated as inhibitors of DHFR from human, *Pneumocystis carinii*, *T. gondii*, rat liver, *Lactobacillus casei*, and *Escherichia coli*, and selected analogues were evaluated as inhibitors of the growth of tumor cells in culture. These analogues displayed potent *T. gondii* DHFR inhibition as well as inhibition of the growth of *T. gondii* cells in culture. Further, selected analogues were potent inhibitors of the growth of tumor cells in culture in the in vitro screening program of the National Cancer Institute with GI_{50}s in the nanomolar and subnanomolar range. Crystallographic data for the ternary complex of hDHFR−NADPH and 2,4-diamino-6-[*N*-(2′,5′-dimethoxybenzyl)-*N*-methylamino]-pyrido[2,3-*d*]pyrimidine, **1c**, reveal the first structural details for a reversed N9−C10 folate bridge geometry as well as the first conformational details of a hybrid piritrexim−trimetrexate analogue.

Infections with *Pneumocystis carinii* and *Toxoplasma gondii* are a major cause of morbidity and mortality in patients with the acquired immunodeficiency syndrome (AIDS).[2] *P. carinii* infections are treated with pentamidine, trimethoprim-dapsone, trimethoprim-sulfamethoxazole, and trimetrexate, while pyrimethamine plus a sulfonamide is used for the treatment of *T. gondii* infections.[3,4] The treatment of *P. carinii* and *T. gondii* infections with nonclassical antifolates such as trimethoprim (TMP), trimetrexate (TMQ), and pyrimethamine

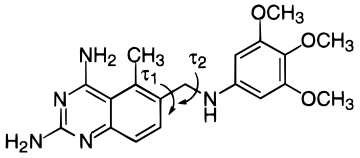

TMQ

takes advantage of the fact that these organisms are permeable to lipophilic, nonclassical antifolates and, unlike mammalian cells, lack the carrier-mediated active transport system(s) required for the uptake of classical antifolates with polar glutamate side chains.[5] In addition, host tissues can selectively be protected by the coadministration of leucovorin (5-formyltetrahydrofolate), which is taken up by mammalian cells and reverses toxicity associated with dihydrofolate reductase (DHFR) inhibitors.[6] Further, these lipophilic agents can penetrate into the central nervous system (CNS) where *T. gondii* infections usually occur.

TMP and pyrimethamine are weak inhibitors of DHFR from *P. carinii* and *T. gondii* and hence have to be used along with sulfonamides to augment their potency.[5] TMQ and piritrexim (PTX), which are 100−

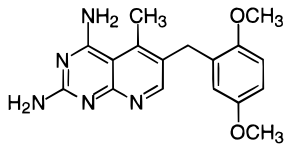

PTX

10 000 times more potent than TMP or pyrimethamine against DHFR from *P. carinii* and *T. gondii*, are also potent inhibitors of mammalian DHFR,[7] and hence their use is associated with significant toxicity. As a result, TMQ has to be coadministered with leucovorin. However, side effects associated with the use of sulfa drugs

† Duquesne University.
‡ Indiana University.
∥ Tufts University.
§ Hauptman-Woodward Medical Research Institute Inc.
⊥ Current address: Abbott Laboratories, Abbott Park, Illinois 60064.

S0022-2623(98)00081-8 CCC: $15.00
Published on Web 08/12/1998

in combination with TMP or pyrimethamine, as well as the high cost of leucovorin, often necessitate discontinuation of therapy.[8] Thus, there is a dire need for new single agents with high potency and selectivity against these organisms. This problem is particularly acute for patients who cannot tolerate existing regimens since, in the absence of a cure for AIDS-infected patients, the prophylactic use of antiopportunistic agents needs to be continued throughout the life of the patient.

As part of a program aimed at identifying potent and selective inhibitors of *P. carinii* and/or *T. gondii* DHFR of diverse structures, we have reported the design and synthesis of a variety of 6−6 ring-fused analogues,[9−11] as well as 6−5 ring-fused analogues,[12,13] with the goal of increasing the selectivity of TMQ and PTX for *P. carinii* (pc)DHFR and *T. gondii* (tg)DHFR. One particularly promising series of compounds recently synthesized by Gangjee et al.[11] was the 2,4-diamino-6-substituted-pyrido[2,3-*d*]pyrimidines of general structure **1**. In these analogues, the normal C9−N10 bridge found

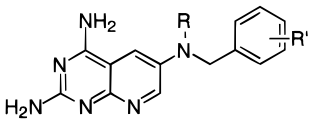

	R	R'
1a.	H	2,5-OCH_3
1b.	H	3,4,5-OCH_3
1c.	H	2,5-OCH_3

in most classical as well as nonclassical DHFR inhibitors was replaced with a reversed N9−C10 bridge. Further, the methyl group at the 5-position which is responsible for increased potency in nonclassical 5-deaza antifolates[9] was transposed to the N9 not only to induce conformational restriction around the bridge geometry τ_1 and τ_2 but also to evaluate hydrophobic interactions of the N9−methyl moiety with DHFR, a feature not explored previously with nonclassical antifolates. Some analogues in the pyrido[2,3-*d*]pyrimidine series were found to possess high potency against pcDHFR and excellent selectivity and potency as inhibitors of tgDHFR, compared to human (h)DHFR, and represent some of the most promising nonclassical antifolates reported to date as candidates against opportunistic infections with *P. carinii* and *T. gondii*.[11] The premise for the synthesis of the 5-desmethyl pyrido[2,3-*d*]pyrimidine analogues **1** was to decrease the activity of these analogues against all DHFR with the contention that perhaps the decrease in inhibitory activity against hDHFR would be greater than the decrease against pcDHFR and/or tgDHFR which would translate into improved selectivity against these organisms versus mammalian cells while maintaining reasonable potency. This hypothesis proved to be correct, and some compounds in the pyrido[2,3-*d*]pyrimidine series were indeed potent and selective against pcDHFR and tgDHFR.[11]

It is well documented from X-ray crystal structures that the 5-methyl moiety of the 5-deaza-5-methyl classical and nonclassical antifolates such as PTX and TMQ make hydrophobic contact with Val115 in hDHFR.[14] Recently the crystal structure of pcDHFR complexed with PTX was published[15] which indicates that the 5-methyl group of PTX is in van der Waals contact with Ile123 of pcDHFR. That 5-methyl analogues are in general more potent than the corresponding 5-desmethyl analogues against DHFR is well documented for both classical[16,17] and nonclassical[9,18] antifolates. The fact that the 5-methyl of PTX makes hydrophobic contact with both pcDHFR and hDHFR is part of the reason that PTX lacks selectivity and is a potent inhibitor of both pcDHFR and hDHFR.

Since 2,4-diamino-6-[*N*-(2′,5′-dimethoxybenzyl)-*N*-methylamino]pyrido[2,3-*d*]pyrimidine, **1c,** was the most selective analogue for pcDHFR from compounds of general structure **1**[11] and was much more potent against pcDHFR (IC_{50} = 84 nM) and tgDHFR (IC_{50} = 28 nM) than hDHFR (IC_{50} = 8500 nM), it was of interest to crystallize this analogue with hDHFR to determine the molecular reason for its low potency against hDHFR and with pcDHFR to determine the reason for its high selectivity. The crystal structure of compound **1c** complexed with hDHFR was determined from cocrystallization experiments, and the results are described in this report for data to 2.1 Å resolution (Figure 1). The crystal structure determination of **1c** with pcDHFR is currently underway.

In the crystal structure of **1c** with hDHFR it is quite evident that the N9−methyl moiety is not in van der Waals contact (≤4.0 Å) with any hydrophobic side chain of hDHFR. This lack of hydrophobic interaction of the N9−methyl moiety of **1c** with the hydrophobic residues of hDHFR in addition to the absence of the 5-methyl moiety and its interaction with Val115 in part accounts for the significantly lower inhibitory potency of **1c** against hDHFR compared to PTX or TMQ which contain a 5-methyl moiety which is capable of hydrophobic contact with hydrophobic residues of hDHFR.[14]

Compound **1c** was modeled on the crystal structure of PTX complexed with pcDHFR,[15] using SYBYL 6.03,[19] in an attempt to determine the structural reason for the increase in potency and for the selectivity of **1c** compared to PTX. Since the X-ray crystal structure coordinates of PTX with pcDHFR are not available, a visual model of the bound conformation of PTX was obtained using the known TMP−pcDHFR coordinates[15] and the superimposition provided in the literature of TMP−pcDHFR and PTX−pcDHFR.[15] The pyrimidine ring of **1c** in the bound conformation, obtained from the crystal structure of **1c** and hDHFR, was superimposed on the pyrimidine ring of PTX bound to pcDHFR.[15] In this model the N9−methyl moiety of **1c** is in van der Waals contact (≤4.0 Å) with both Ile123 and Ile65 of pcDHFR. These additional hydrophobic interactions of **1c** with pcDHFR compared to the lack of hydrophobic interactions of the N9−methyl moiety of **1c** with hDHFR as observed in the crystal structure could account, in part, for both the increased potency and selectivity of **1c** for pcDHFR compared with hDHFR.

In light of its excellent potency and selectivity, compound **1c** was evaluated as an inhibitor of the growth of *T. gondii* cells in culture. The cell culture/enzyme IC_{50} ratio (447) for *T. gondii* indicated a greater than 400-fold decrease in inhibition of the growth of cells in culture compared with inhibition of the enzyme. This suggests a lack of adequate cell penetration in *T. gondii* cells in culture. Despite its poor cell culture/enzyme IC_{50} ratio, compound **1c** did show oral activity when

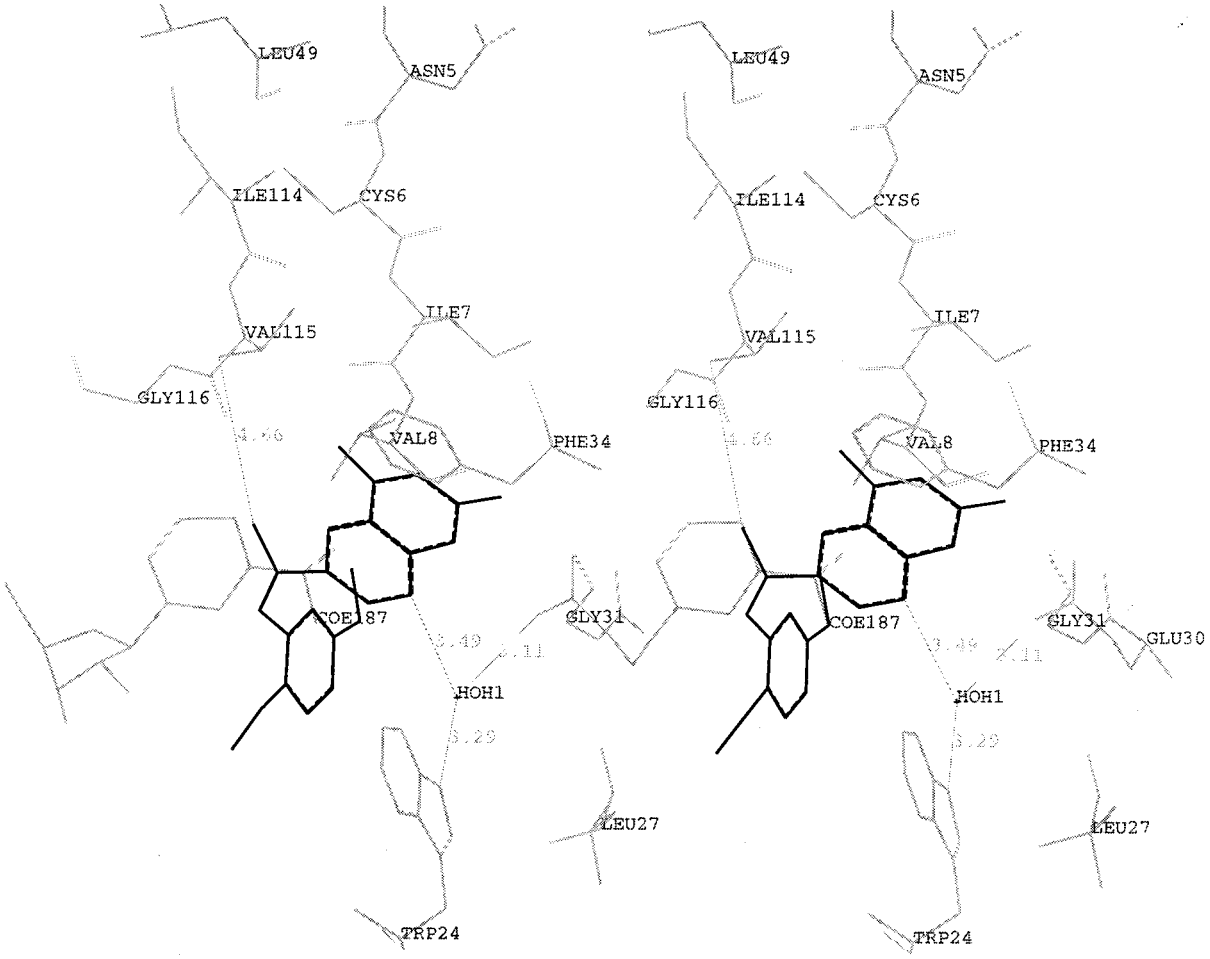

Figure 1. Stereodiagram showing the X-ray crystal structure of **1c** (dark) in hDHFR F31G variant with NADPH (COE187). The water molecule HOH1 is shown hydrogen bonded to Glu30 (3.11 Å), Trp24 (3.29 Å), and the N8 of **1c** (3.49 Å). The distance between the N9−CH_3 and Val 115 is also designated (4.66 Å).

tested in the mouse model for *T. gondii* infection.[11] However, improvement in the cell culture/enzyme IC_{50} ratio could provide significant improvement in in vivo activity. It was therefore of interest to maintain the structural features of compound **1c** for potency and selectivity and to concomitantly increase the lipid solubility to provide for better inhibition of the growth of cells in culture. We elected to achieve this goal by isosterically replacing the N8 of pyrido[2,3-*d*]pyrimidines **1** with a carbon atom to afford quinazolines. We have demonstrated that calculated log *P* values can be used to predict enhanced inhibition of the growth of cells in culture of a number of similar antifolates.[20] Log *P* calculations indicated that analogues in the reversed bridge quinazoline series had significantly improved log *P* values compared to those of the corresponding compounds in the pyrido[2,3-*d*]pyrimidine series as shown in Table 4 which were anticipated to provide better *P. carinii* and *T. gondii* cell inhibition. Thus we designed and synthesized the reverse bridge quinazoline series **2**−**15** (Table 1) where the N8−nitrogen of compounds

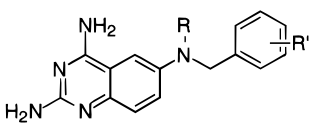

2-15

1 was replaced by a CH.

Table 1

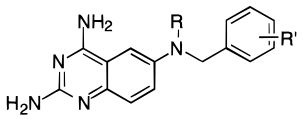

	R	R′
2	H	H
3	H	2,5-OCH_3
4	H	3,5-OCH_3
5	H	2,4-OCH_3
6	H	3,4,5-OCH_3
7	H	2,3,4-OCH_3
8	H	2,4,5-OCH_3
9	H	2,4,6-OCH_3
10	H	2,3-C_4H_4
11	CH_3	2,5-OCH_3
12	CH_3	3,5-OCH_3
13	CH_3	2,4-OCH_3
14	CH_3	2,3,4-OCH_3
15	CH_3	2,3-C_4H_4

Molecular modeling using SYBYL 6.03[19] and superimposing the low-energy conformations of 2,4-diamino-6-substituted quinazolines on the crystal structure of **1c** with hDHFR and on the crystal structure of PTX with pcDHFR lent further credence to the rationale that these quinazolines with the N9−methyl substitution should bind much like compound **1c** and hence should provide the selectivity and potency demonstrated by **1c**. Thus analogues **2**−**15** and in particular **11**−**15** were

Scheme 1[a]

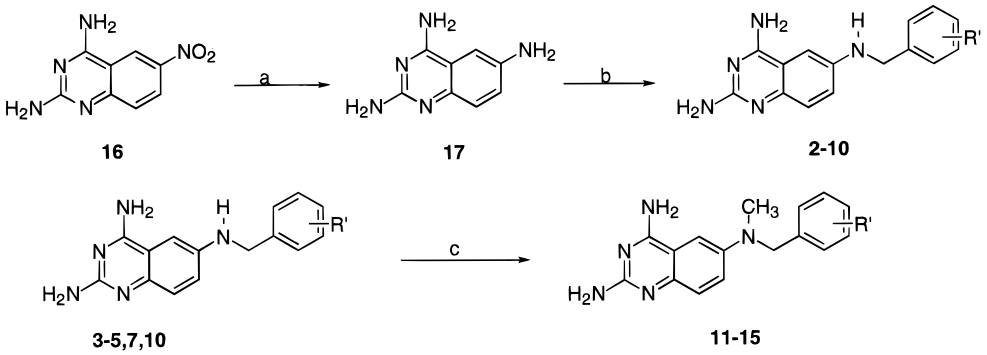

[a] Reagents: (a) Raney nickel/DMF/H_2 30 psi; (b) Raney nickel/DMF/AcOH/ArCHO/H_2 30 psi; (c) HCHO/$NaCNBH_3$/HCl.

anticipated to combine the potency and selectivity of **1** with significantly improved inhibition of the growth of cells in culture. Such analogues could be used as single agents or with much lower doses of sulfa drugs which would overcome some of the drawbacks of currently used DHFR inhibitors in the treatment of opportunistic infections caused by *P. carinii* and *T. gondii*.

In addition, since 2,4-diaminoquinazolines such as TMQ have been involved in phase II clinical trials as antitumor agents, it was also of interest to evaluate analogues **2**−**15** as potential antitumor agents. Clearly those analogues which were significantly selective for *P. carinii* and/or *T. gondii* DHFR were not anticipated to function as potent inhibitors of the growth of tumor cells in culture.

Chemistry

The target compounds **2**−**15** were synthesized (Scheme 1) from commercially available 2,4-diamino-6-nitroquinazoline **16** which was reduced with Raney nickel and hydrogen at 30 psi, to afford the key intermediate 2,4,6-triaminoquinazoline **17**. The appropriate benzaldehyde or naphthaldehyde was then reductively aminated with **17** under hydrogen at 30 psi, to afford target compounds **2**−**10** in yields ranging from 26 to 61%. Reductive methylation of **3**, **4**, **5**, **7**, and **10**, using formaldehyde and sodium cyanoborohydride at a pH of 2−3, regiospecifically afforded the corresponding N9−methyl analogues **11**−**15** in yields ranging from 89 to 95%.

X-ray Crystal Structure

The overall characteristics of the hDHFR ternary complex with NADPH and **1c** are similar to those reported for other hDHFR complexes, and the binding orientation of the analogue **1c** is similar to that observed for PTX and TMQ.[21] The carboxylate oxygens of Glu30 interact with the pyridopyrimidine ring forming contacts with the N1 nitrogen by OE2 and OE1 to the 2-NH_2 nitrogen. In addition, the carboxylate oxygen OE1 of Glu30 forms a hydrogen bond to the hydroxyl of Thr136, which in turn interacts with a conserved water and also with the 2-NH_2 group of **1c**. There is a further hydrogen-bonding network formed by another conserved water molecule which forms contacts with OE2 of Glu30, the N8 nitrogen of **1c**, and NE1 of Trp24. These patterns have been observed in most DHFR crystal structures.[21−23]

These data provide the first structural observation of a reversed N9−C10 bridge in normal folate analogues and also the first structural details for a hybrid molecule containing key features of PTX and TMQ. As illustrated in Figure 1, the reversal of this bridge places the N9−methyl in a pocket of the hDHFR active site not occupied by any other class of antifolate analogues. In this orientation, the N9−methyl group does not make any contacts within the range of <4 Å of the hydrophobic residues Thr56, Ile60, Val115, or the nicotinamide ring carbon. This lack of interaction of the N9−methyl moiety of **1c** with the hydrophobic residues of hDHFR, in addition to the absence of the 5-methyl moiety, in part, accounts for the significantly lower potency of **1c** against hDHFR compared to TMQ or PTX which contain a 5-methyl moiety and are capable of significant contact with hydrophobic residues of hDHFR.

Modeling studies of this compound in the active site of pcDHFR made by a least-squares fit of the backbone structure pcDHFR from the furopyrimidine ternary complex[24] to this structure reveals that there are similar hydrophobic contacts present; however, they are more compact than in this human structure. In addition, the substitution of Val115 in hDHFR by Ile123 in pcDHFR permits closer intermolecular hydrophobic contacts to be made via the N9−methyl moiety of **1c** and pcDHFR and could account for part of the enhanced potency observed for this analogue against pcDHFR.

Biological Activity and Discussion

Analogues **2**−**15** were evaluated as inhibitors of pcDHFR,[25] tgDHFR,[26] and rat liver (rl)DHFR, and the results (IC_{50}) are reported in Table 2. Selectivity ratios (IC_{50} rlDHFR/IC_{50} pcDHFR and IC_{50} rlDHFR/IC_{50} tgDHFR) were determined using rlDHFR as the mammalian source and are also reported in Table 2. The choice of side chain substituents for these quinazoline analogues was based on the potent and selective pyrido[2,3-*d*]-pyrimidine series reported by Gangjee et al.[11] Comparison of the inhibitory activity of analogues **3**−**9** with **2** (Table 2) indicates that introduction of methoxy groups in the side chain phenyl ring slightly improves inhibition of pcDHFR and tgDHFR except for **9**, the only compound in the group with diortho substitution. The rlDHFR inhibitory potency decreases slightly on addition of methoxy groups on the side chain phenyl ring; thus, analogues **2**−**9** were selective inhibitors of tgDHFR versus rlDHFR. Despite the differential change in the inhibition of pcDHFR and rlDHFR on introduction of methoxy groups, selective inhibitors of pcDHFR were not obtained.

Table 2. Inhibitory Concentrations (IC_{50}) in μM and Selectivity Ratios of **2**−**15** against *P. carinii* (pc), *T. gondii* (tg), and Rat Liver (rl)DHFR[a]

	pc	rl	rl/pc	tg	rl/tg
2	8.7	0.66	0.08	0.32	2.1
3	4.6	1.1	0.24	0.16	6.88
4	2.2	0.84	0.38	0.12	7
5	4.4	1.2	0.27	0.17	7.1
6	6.8	0.9	0.13	0.084	10.7
7	4.9	1.3	0.27	0.19	6.8
8	5.4	1.6	0.29	0.124	12.9
9	116	22.7	0.19	0.95	23.9
10	0.72	0.19	0.26	0.099	1.9
11	0.087	0.026	0.29	0.03	0.86
12	0.0238	0.0082	0.34	0.0093	0.88
13	0.10	0.043	0.43	0.039	1.1
14	0.052	0.019	0.36	0.017	1.1
15	0.017	0.017	1	0.021	0.80
TMQ[b]	0.042	0.003	0.07	0.01	0.3
TMP[b]	12	133	11.1	2.7	49

[a] These assays were carrried out at 37 °C under saturating conditions of substrate (90 μM dihydrofolic acid) and cofactor (119 μM NADPH); tgDHFR and rlDHFR were assayed in the presence of 150 mM KCl.[25,26] [b] Data from ref 11.

Introduction of a 2,4,6-trimethoxy substituent in the side chain phenyl (compound **9**) results in a 13-, 3-, and 26-fold decrease in the inhibition of pcDHFR, tgDHFR, and rlDHFR, respectively, compared with **2**. A comparison of the inhibitory activity of **5** (2,4-diOCH_3 Ph) and **9** (2,4,6-triOCH_3Ph) illustrates the detrimental effect on DHFR inhibition with the introduction of an additional ortho methoxy moiety on the phenyl ring. This decreased activity of **9** could be attributed to an intolerance of the enzyme for diortho substituents and/or a change in the conformation of the side chain phenyl ring, resulting from the bulk of a diortho substitution which is not conducive to binding. As a result of its significantly diminished rlDHFR potency compared to tgDHFR, analogue **9** displayed a 23-fold selectivity for tgDHFR and was the most selective inhibitor of tgDHFR in this entire series versus rlDHFR. In addition the decrease in DHFR inhibitory activity with a 2,4,6-trimethoxy-substituted phenyl was the least for tgDHFR, indicating a greater tolerance for di-orthomethoxy substituents.

On the basis of their superior selectivity toward tgDHFR, compounds **6**, **8**, and **9** were tested as inhibitors of the growth of *T. gondii* cells in culture; the IC_{50} values were 12, 11, and 3 μM, respectively. Thus the IC_{50} *T. gondii* cell culture/IC_{50} tgDHFR ratio for **6**, **8**, and **9** was 142, 89, and 3, respectively, which was significantly better than the ratio of 447 for the pyrido[2,3-*d*]pyrimidine **1c**. For comparison, the IC_{50} value for pyrimethamine in the same assay was 0.64 μM.[26]

Replacement of the phenyl ring of compound **2** with a 1-naphthyl moiety (**10**) provided interesting results. The activity against all three DHFR was increased. The active site of hDHFR has been shown to be large enough to accommodate a naphthyl ring in the side chain;[27] hence the increased inhibition of rlDHFR with a naphthalene side chain was not unexpected. The increased inhibition of pcDHFR and tgDHFR as well by analogue **10** suggests that the size of the active sites of pcDHFR and tgDHFR are also large enough to accommodate a naphthyl moiety. However the selectivity for pcDHFR and tgDHFR was not improved compared to the phenyl unsubstituted analogue **2**.

N9−methylation of compounds **3**−**5**, **7**, and **10** to afford **11**−**15**, respectively, results in a significant increase in inhibition of all three DHFR. Thus, N9−methylation of **3** to afford **11** results in a 53-, 5-, and 42-fold increase in inhibition of pcDHFR, tgDHFR, and rlDHFR, respectively. However, as a result of the greater increase in the inhibition of rlDHFR, its selectivity against tgDHFR was decreased. N9−methylation of **4** to afford **12** resulted in a 92-, 13-, and 102-fold increase in the inhibition of pcDHFR, tgDHFR, and rlDHFR, respectively, and provided the most potent inhibitor of tgDHFR and rlDHFR of the entire series of compounds in this study. Compound **12** is as potent as TMQ against pcDHFR and tgDHFR. N9−methylation of **5** affords **13** which shows a 44-, 4-, and 28-fold increase in inhibition of pcDHFR, tgDHFR, and rlDHFR, respectively. The differential increase in DHFR inhibition indicates that the active site of pcDHFR and tgDHFR are quite different, in particular with respect to the interaction of the N9−methyl moiety with the enzymes and/or the effect of the N9−methyl group on the conformation of the bridge and the side chain phenyl ring. Comparison of the inhibition profiles of compounds **5** and **7**, and **13** and **14**, suggests that the addition of the third methoxy group does not afford a beneficial effect for the inhibition of pcDHFR or tgDHFR, implying that it does not interact with any residue in the active site. This information could be used to impart beneficial properties to these molecules such as improved solubility using substituents at this site for the inhibition of *P. carinii* and/or *T. gondii* cells in culture.

A comparison of the activities and selectivities (versus rlDHFR) of these quinazoline analogues with the pyrido[2,3-*d*]pyrimidines[11] with identical side chain substituents reveals some differences. In the latter series, the N9−methyl-2′,5′-diOCH_3Ph analogue **1c** was among the most potent and selective against tgDHFR, and for the other analogues, N9−methylation did not change the selectivity. In contrast, the most selective analogues in the quinazoline series were the N9−H analogues, and contrary to the pyrido[2,3-*d*]pyrimidines, N9−methylation of the quinazolines abolished selectivity. These N9−H quinazoline analogues were, in general, more selective for tgDHFR than the corresponding pyrido[2,3-*d*]pyrimidines. With a few exceptions, the quinazolines were also more potent than the pyrido[2,3-*d*]pyrimidines.

Analogues **2**−**15** were also evaluated against human (h)DHFR, *Escherichia coli* (ec)DHFR, *Lactobacillus casei* (lc)DHFR, as well as recombinant tgDHFR, under slightly different assay conditions,[28] and the results are reported in Table 3, along with selectivity ratios versus hDHFR. TMP and TMQ are included for comparison. N9−methylation resulted in a dramatic increase in the inhibition of hDHFR (as was observed for rlDHFR). Thus the N9−methyl analogues **11** and **12** were 1077- and 2545-fold more potent against hDHFR than the corresponding N9−H compounds **3** and **4**, respectively. The inhibition of tgDHFR was also significantly increased on N9−methylation, with **11** and **12** being 282- and 179-fold more potent than **3** and **4**, respectively. Several analogues were identified as selective inhibitors of tgDHFR with selectivity ratios of 1.7−33. Further,

Table 3. Inhibitory Concentrations (IC_{50}) in μM and Selectivity Ratios of Analogues **2**−**15** against Human (h)DHFR, *T. gondii* (tg)DHFR, *E. coli* (ec)DHFR, and *L. casei* (lc)DHFR[a]

	hDHFR	tgDHFR	h/tg	ecDHFR	h/ec	lcDHFR	h/lc
2	2.4	1.4	1.7	0.51	4.7	2.7	0.9
3	28	1.1	25	0.42	67	3.0	9.3
4	28	0.84	33	0.42	67	2.3	12.2
5	26	0.78	33	0.39	67	2.1	12.4
6	23	0.92	25	0.23	100	2.8	8.2
7	27	0.81	33	0.41	66	2.0	13.5
8	1.4	0.54	2.6	0.14	10	1.6	0.9
9	25	0.75	33	1.0	25	37	0.7
10	0.6	0.09	6.6	0.15	4	1.8	0.3
11	0.026	0.0039	6.6	0.0078	3.3	0.13	0.2
12	0.011	0.0047	2.3	0.0028	3.9	0.037	0.3
13	0.05	0.0039	12.8	0.013	3.8	0.12	0.4
14	0.14	0.0054	26	0.0081	17	0.059	2.4
15	0.027	0.0041	6.6	0.0054	5	0.021	1.3
TMP	340	6.8	50	0.01	34000	0.26	1308
TMQ	0.054	0.0072	7.5	0.018	3.0	0.054	1.0

[a] Recombinant hDHFR was provided by Dr. J. H. Freisheim. Recombinant tgDHFR was provided by Dr. D. V. Santi. Recombinant ecDHFR was provided by Dr. R. L. Blakley. DHFR assay conditions:[28] all enzymes were assayed spectroscopically in a solution containing 50 μM dihydrofolate, 80 μM NADPH, 0.05 μM Tris HCl, 0.001 M 2-mercaptoethanol, and 0.001 M EDTA at pH 7.4 and 30 °C. The reaction was initiated with an amount of enzyme yielding a change in o.d. at 340 nm of 0.015/min.

Table 4. Comparison of the HDHFR and TgDHFR Inhibition (IC_{50}) in μM and Calculated log *P* Values of **3**, **6**, **11**, and **12** with the Corresponding Pyrido[2,3-*d*]pyrimidines **1a**−**1d**[11]

	hDHFR	tgDHFR	h/tg	log P[a]
3	28	1.1	25	2.35
1a (R = H; R′ = 2,5-OCH_3)	13	0.5	26	1.32
6	23	0.92	25	1.91
1b (R = H; R′ = 3,4,5-OCH_3)	76	0.395	192	0.89
11	0.026	0.0039	6.6	2.90
1c (R = CH_3; R′ = 2,5-OCH_3)	8.5	0.028	304	1.87
12	0.01	0.0047	2.3	2.90
1d (R = CH_3; R′ = 3,5-OCH_3)	2.9	0.029	100	1.87

[a] Calculated using log K_{OW}—estimation of log octanol/water partition coefficient version 1.03—Syracuse Research Corporation.

analogues **11**−**15** were as potent as TMQ against tgDHFR with equivalent or better selectivities. However, the remarkable selectivities observed against tgDHFR with the pyrido[2,3-*d*]-pyrimidines, some as high as 300-fold,[11] were absent in the quinazoline series. The selectivities and potencies against ecDHFR were in general slightly greater for the N9−H analogues and slightly lower for the N9−methyl analogues compared to their effect on tgDHFR. Against lcDHFR the analogues were less potent and selective compared to their activities against tgDHFR.

Since compounds **2**−**15** were designed on the basis of the previously synthesized pyrido[2,3-*d*]pyrimidines[11] with the objective of increasing cell penetration, it was of interest to determine the effects of the replacement of the nitrogen (N8 of a pyrido[2,3-*d*]pyrimidine) with a carbon (C8 of a quinazoline) on DHFR inhibition. A comparison of the hDHFR and tgDHFR inhibitory activities along with selectivity ratios of four quinazolines **3**, **6**, **11**, and **12** synthesized in this study, with the previously synthesized pyrido[2,3-*d*]pyrimidines **1a**−**d**,[11] respectively, and with identical substituents on the side chain, are listed in Table 4. With the exception of **3** and **1a**, the hDHFR inhibition results indicate that the quinazoline analogues are more potent than the corresponding pyrido[2,3-*d*]pyrimidines. This effect is augmented on N9−methylation where the quinazoline analogues **11** and **12** are 327- and 290-fold more potent against hDHFR than the corresponding pyrido[2,3-*d*]-pyrimidines **1c** and **1d**, respectively. However, compounds **11** and **12** were only 6-fold more potent as inhibitors of tgDHFR than the corresponding pyrido-[2,3-*d*]pyrimidines. These results indicate that the presence of a quinazoline moiety is much more conducive to potent inhibition of hDHFR than to tgDHFR when compared with the corresponding pyrido[2,3-*d*]-pyrimidines. It is this increased inhibition of hDHFR that is responsible for the considerable loss of selectivity against tgDHFR for the quinazolines.

The significant and selective augmentation of hDHFR inhibition, attributed to the N9−methyl moiety of the quinazolines as compared to the pyrido[2,3-*d*]pyrimidines (shown in Table 4), could result from a conformational effect that positions the N9−methyl moiety in the quinazolines to interact with residues on hDHFR as well as other DHFR. This conformational positioning of the N9−methyl moiety is probably not possible to the same extent in the pyrido[2,3-*d*]pyrimidines, possibly due to the N8−nitrogen. The N8−nitrogen in the pyrido[2,3-*d*]pyrimidines has been shown to interact through a hydrogen bridge via a conserved water molecule to Glu30 and Trp24 in hDHFR, thus restricting the ability to position the N9−methyl in a conducive orientation in hDHFR. Similar hydrogen bonding with a water molecule in hDHFR has been observed for the classical antitumor agent methotrexate and PTX.[14,23] This could also explain, in part, the different structure−activity and selectivity profiles observed with quinazoline analogues **2**−**15** as compared with the corresponding pyrido[2,3-*d*]pyrimidines, since compounds with identical side chains differ only in the substitution at the 8-position in the two series. This hypothesis is partially validated from the crystal structure of the pyrido[2,3-*d*]pyrimidine analogue **1c** with hDHFR as shown in Figure 1, which indicates no van der Waals or hydrophobic contact of the N9−methyl moiety with Ile114 or Val115, thus accounting in part for its lower inhibitory activity against hDHFR compared to other DHFRs. In addition, the presence of a water molecule which interacts with the N8−nitrogen (Figure 1) and provides a bridge to Glu30 and Trp24 in hDHFR also restricts the positioning of the *N*−methyl moiety as suggested previously. Thus, the lack of high selectivity in the quinazolines synthesized in this study as compared to that of the pyrido[2,3-*d*]pyrimidines could arise, in part, from a productive hydrophobic interaction of the N9−methyl moiety of the quinazolines with hDHFR as well as other DHFR. In addition, the conformational effects of N9−methylation on the relative positioning of the heterocyclic, as well as the phenyl ring and the bridge, could play an important role in the lack of high selectivity of these quinazoline analogues. Confirmation of these hypotheses must await the crystal structures of **11** with pcDHFR and hDHFR which is currently underway.

The significant hDHFR inhibition of these quinazoline analogues prompted their selection by the National Cancer Institute in the antitumor in vitro preclinical screening program.[29] The remarkable increment in hDHFR inhibition on N9−methylation was reflected in

the superior cytotoxicity of the N9−methyl analogues as compared to the corresponding N9−H analogues. Compounds **11**, **12**, and **14** displayed potent inhibitory activity against the growth of various tumor cell lines in culture with $GI_{50} < 10^{-8}$ M. The cytotoxic properties of these compounds can be attributed to their excellent hDHFR inhibition.

In summary, several potent and selective inhibitors of tgDHFR have been synthesized in this study. The goal of this work was to improve the cell penetration of highly selective pyrido[2,3-*d*]pyrimidines synthesized previously, while maintaining their potency and selectivity. This goal was partially achieved, as the synthesized quinazolines had considerably improved calculated lipophilicity parameters and a decrease in the IC_{50} *T. gondii* cell culture/IC_{50} tgDHFR inhibitory ratio compared to **1c** as well as high activity against tumor cells in culture. However, the replacement of the N8−nitrogen in pyrido[2,3-*d*]pyrimidines with a carbon in the quinazolines resulted in an unanticipated loss of the excellent selectivity achieved with the pyrido[2,3-*d*]-pyrimidines. As a result, alternate strategies to improve the cell penetration of the pyrido[2,3-*d*]pyrimidine analogues are currently underway and will be the subject of future communications. Several of the analogues synthesized in this study displayed exceptional cytotoxic properties in the preclinical in vitro antitumor screening program of the National Cancer Institute. The potencies of these compounds against the growth of a wide range of tumor cell lines in culture warrants their further evaluation as antitumor agents. The goal of developing antifolates as potent and selective inhibitors of pcDHFR and tgDHFR with good cell penetration, however, remains a challenge and in light of the AIDS pandemic continues to be a worthwhile goal.

Experimental Section

Melting points were determined on a Fisher-Johns melting point apparatus or a Mel Temp apparatus and are uncorrected. Nuclear magnetic resonance spectra for proton (^{1}H NMR) were recorded on a Brucker WH-300 (300 MHz). The data were accumulated by 16K size with 0.5 s delay time with internal standard tetramethylsilane; s = singlet, br s = broad singlet, d = doublet, t = triplet, q = quartet, m = multiplet. Thin layer chromatography (TLC) was performed on silica gel plates with fluorescent indicator and were visualized with light at 254 and 366 nm, unless indicated otherwise. Column chromatography was performed with 230−400 mesh silica gel purchased from Aldrich Chemical Co., Milwaukee, Wisconsin. Elution was performed using a gradient, and 10 mL fractions were collected, unless mentioned otherwise. All anhydrous solvents were purchased from Aldrich Chemical Co. and were used without further purification. Samples for micro analysis were dried in vacuo over phosphorus pentoxide at 70 or 110 °C. Fractional moles of water or organic solvents, frequently found in some analytical samples of the antifolates, could not be prevented despite drying in vacuo and were confirmed by their presence in the ^{1}H NMR spectrum. Microanalyses were performed by Atlantic Microlabs, Norcoss, Georgia.

Procedure A: General Procedure for the Synthesis of Compounds 2−10. 2,4-Diamino-6-nitroquinazoline (1 equiv) was dissolved in 100 mL of *N*,*N*-dimethylformamide with warming (75 °C). To this solution was added Raney nickel (1.0 g), and the mixture was hydrogenated in a Parr hydrogenation apparatus at 35 psi and room temperature for 3 h. TLC analysis ($CHCl_3$:CH_3OH:NH_4OH 5:2:1 drop) indicated absence of starting material and the appearance of a new spot, corresponding to 2,4,6-triaminoquinazoline. The appropriate benzaldehyde (1.2 equiv) was then added, followed by the addition of 10−15 mL of glacial acetic acid, and the mixture was further hydrogenated for 6−7 h at 35 psi and room temperature. TLC analysis ($CHCl_3$:CH_3OH:NH_4OH 5:2:1 drop) indicated the presence of a new product along with some unreacted 2,4,6-triaminoquinazoline. The reaction was filtered through a Celite pad, and the pad was washed repeatedly with DMF until the washings were colorless. Silica gel (1.0 g) was added to the filtrate, and the solvents evaporated (40 °C, 0.1 mmHg) to afford a dry plug. This plug was applied on the surface of a 1.05 in. × 23 in. silica gel column and eluted with $CHC1_3$:CH_3OH using a gradient elution (95:5 to 80:20). Fractions containing pure product (TLC) were pooled and evaporated to afford analytically pure compound.

Procedure B: General Procedure for the Preparation of Compounds 11−15. To 2,4-diamino-6-[(N-substituted-benzyl)amino]quinazoline (0.l g, 0.48 mmol) in 25 mL of acetonitrile was added formaldehyde (0.04 g, 1.l mmol) with constant stirring. To this suspension was added sodium cyanoborohydride (0.05 g, 0.84 mmol), and the pH of the mixture was adjusted to 2−3 using concentrated HCl. The starting material initially went into solution at pH 2−3, and after 5 min a bright yellow precipitate was obtained. TLC ($CHCl_3$:CH_3OH:NH_4OH-5:2:0.5) showed the presence of a new spot with the absence of the starting material spot. The acetonitrile was evaporated under reduced pressure and the residue obtained was suspended in 10 mL of water. This suspension was neutralized using NH_4OH to afford the N9−methyl derivative of the appropriate 2,4-diamino-6-[(N-substituted-benzyl)amino]quinazoline.

2,4-Diamino-6-[N-(benzyl)amino]quinazoline, 2. Compound **2** was synthesized from 2,4-diamino-6-nitroquinazoline (0.50 g, 2.43 mmol) and benzaldehyde (0.57 g, 2.91 mmol) to afford after purification 0.43 g (55%) of **2** as a bright yellow powder: mp 177.3 °C; TLC R_f 0.53 ($CHCl_3$:CH_3OH:NH_4OH-5:2:0.5); ^{1}H NMR (DMSO-d_6) δ 4.29 (d, 2 H, 10-CH_2), 5.86 (s, 2 H, 4-NH_2), 5.99 (d, 1 H, 9-NH), 6.98−7.43 (m, 10 H, Ar, 2-NH_2). Anal. calcd for ($C_{l5}H_{l5}N_5$·0.5CH_3COOH) C, H, N.

2,4-Diamino-6-[*N*-(2′,5′-dimethoxybenzyl)amino]quinazoline, 3. Compound **3** was synthesized from 2,4-diamino-6-nitroquinazoline (0.50 g, 2.43 mmol) and 2,5-dimethoxybenzaldehyde (0.60 g, 3.65 mmol) using procedure A to afford after purification 0.18 g (23.29%) of **3** as a yellow solid: mp 171−172 °C; TLC R_f 0.57 ($CHCl_3$:CH_3OH:NH_4OH-5:2:0.5); ^{1}H NMR (DMSO-d_6) δ 3.64 (s, 3 H, OCH_3), 3.77 (s, 3 H, OCH_3), 4.23 (d, 2 H, 10-CH_2), 5.90 (t, 1 H, 9-NH), 6.34 (s, 2 H, 4-NH_2), 6.78 (t, 1 H, Ar), 6.92 (t, 2 H, Ar), 7.09 (m, 3 H, 5,7,8-CH), 7.66 (s, 2 H, 2′-NH_2). Anal. calcd for ($C_{17}H_{19}N_5O_2$·0.5H_2O·0.4CH_3COOH) C, H, N.

2,4-Diamino-6-[*N*-(3′,5′-dimethoxybenzyl)amino]quinazoline, 4. Compound **4** was synthesized from 2,4-diamino-6-nitroquinazoline (0.50 g, 2.43 mmol), and 3,5-dimethoxybenzaldehyde (0.45 g, 2.68 mmol) using procedure A to afford after purification 0.50 g (63%) of **4** as a light yellow solid: mp 182−183 °C; TLC R_f 0.61 ($CHCl_3$:CH_3OH:NH_4OH-5:2:0.5); ^{1}H NMR (DMSO-d_6) δ 3.70 (s, 6 H, 3′,5′-OCH_3), 4.20 (d, 2 H, 10-CH_2), 5.85 (s, 2 H, 4-NH_2), 6.00 (t, 1 H, 9-NH_2), 6.34 (m, 1 H, −Ar), 6.59 (s, 2 H, Ar), 7.04 (m, 3 H, 5,7,8-CH), 7.14 (s, 2 H, 2-NH_2). Anal. calcd for ($C_{17}H_{19}N_5O_2$·0.5CH_3COOH) C, H, N.

2,4-Diamino-6-[*N*-(2′,4′-dimethoxybenzyl)amino]quinazoline, 5. Compound **5** was synthesized from 2,4-diamino-6-nitroquinazoline (0.50 g, 2.43 mmol) and 2,4-dimethoxybenzaldehyde (0.45 g, 2.68 mmol) using procedure A to afford after purification 0.25 g (32%) of **5** as a light brown solid: mp 204−205 °C; TLC R_f 0.59 ($CHCl_3$:CH_3OH:NH_4OH-5:2:0.5); ^{1}H NMR (DMSO-d_6) δ 3.70 (s, 3H, OCH_3), 3.79 (s, 3 H, OCH_3), 4.16 (d, 2 H, 10-CH_2), 5.67 (t, 1 H, 9-NH), 5.92 (s, 2 H, 4-NH_2), 6.70 (d, 1 H, Ar), 7.05 (m, 4 H, Ar), 7.28 (s, 2 H, 2NH_2). Anal. calcd for ($C_{17}H_{19}N_5O_2$·0.5H_2O·0.7CH_3COOH) C, H, N.

2,4-Diamino-6-[*N*-(3′,4′,5′-trimethoxybenzyl)amino]quinazoline, 6. Compound **6** was synthesized from 2,4-diamino-6-nitroquinazoline (0.50 g, 2.43 mol), and 3,4,5-trimethoxybenzaldehyde (0.70 g, 3.65 mmol) using procedure A to afford after purification 0.38 g (44%) of **6** as a bright yellow solid: mp 193−194 °C; TLC R_f 0.52 ($CHCl_3$:CH_3OH:NH_4OH-5:2:0.5);

^{1}H NMR (DMSO-d_6) δ 3.61 (s, 3 H, 4′-OCH_3), 3.74 (s, 6 H, 3′,5′-OCH_3), 4.20 (d, 2 H. 10-CH_2), 6.08 (t, 1 H, 9-NH), 6.17 (s, 2 H, 4-NH_2), 6.77 (s, 2 H, 2′, 6′-CH), 7.08 (d, 3 H, 5,7,8-CH), 7.45 (s, 2 H, 2NH_2). Anal. calcd for ($C_{18}H_{21}N_5O_3$·0.7H_2O·1.1CH_3-COOH) C, H, N.

2,4-Diamino-6-[*N*-(2′,3′,4′-trimethoxybenzyl)amino]quinazoline, 7. Compound **7** was synthesized from 2,4-diamino-6-nitroquinazoline (0.50 g, 2.43 mmol) and 2,3,4-trimethoxybenzaldehyde (0.57 g, 2.91 mmol) using procedure A to afford after purification 0.23 g (27%) of **7** as a yellow solid: mp 213−214 °C; TLC R_f 0.49 ($CHCl_3$:CH_3OH:NH_4OH-5: 2:0.5); ^{1}H NMR (DMSO-d_6) δ 3.75 (s, 6 H, OCH_3), 3.76 (s, 3 H, OCH_3), 4.16 (d, 2 H, 10-CH_2), 5.59 (t, 1 H, 9-NH), 5.70 (s, 2 H, 4-NH_2), 6.76 (d, 1 H, Ar), 7.04−7.11 (m, 6 H, Ar, 2-NH_2). Anal. calcd for ($C_{18}H_{21}N_5O_3$·0.2CH_3COOH) C, H, N.

2,4-Diamino-6-[*N*-(2′,4′,5′-trimethoxybenzyl)amino]quinazoline, 8. Compound **8** was synthesized from 2,4-diamino-6-nitroquinazoline (0.50 g, 2.43 mmol) and 2′,4′,5′-trimethoxybenzaldehyde (0.57 g, 2.92 mmol) using procedure A to afford after purification 0.28 g (32%) of **8** as a yellowish white solid: mp 195−196 °C; TLC R_f 0.52 ($CHCl_3$:CH_3OH:NH_4OH-5:2:0.5); ^{1}H NMR (DMSO-d_6) δ 3.61 (s, 3 H, OCH_3), 3.74 (s, 3H, OCH_3), 3.77 (s, 3 H, OCH_3), 4.10 (d, 2 H, 10-CH_2), 5.46 (t, 1 H, 9-NH), 5.57 (s, 2 H, 4-NH_2), 6.66 (s, 1 H, Ar), 7.02 (m, 6 H, Ar, 2-NH_2). Anal. calcd for ($C_{18}H_{21}N_5O_3$·0.25CH_3COOH) C, H, N.

2,4-Diamino-6-[*N*-(2′,4′,6′-trimethoxybenzyl)amino]quinazoline, 9. Compound **9** was synthesized from 2,4-diamino-6-nitroquinazoline (0.50 g, 2.43 mmol) and 2,4,6-trimethoxybenzaldehyde (0.57 g, 2.91 mmol) using procedure A to afford after purification 0.34 g (39%) of **9** as a brownish green solid: mp 193−194 °C; TLC R_f 0.55 ($CHCl_3$:CH_3OH:NH_4OH-5:2:0.5); ^{1}H NMR (DMSO-d_6) δ 3.77(m, 9 H, 2′,4′,6′-OCH_3), 4.05 (s, 2 H, 10-CH_2), 5.04 (s, 1 H, 9-NH), 5.99 (s, 2 H, 4-NH_2), 6.26 (s, 2 H, 3′,5′-CH), 7.05 (m, 3 H, 5,7,8-CH). Anal. calcd for ($C_{18}H_{21}N_5O_3$·0.4H_2O·0.55CH_3COOH) C, H, N.

2,4-Diamino-6-[*N*-(1′-naphthylmethylene)amino]quinazoline, 10. Compound **10** was synthesized from 2,4-diamino-6-nitroquinazoline (0.50 g, 2.43 mmol) and 1-naphthaldehyde (0.46 g, 2.92 mmol) using procedure A to afford after purification 0.40 g (53%) of **10** as a yellow solid: mp 214−215 °C; TLC R_f 0.47 ($CHCl_3$:CH_3OH:NH_4OH-5:2:0.5); ^{1}H NMR (DMSO-d_6) δ 4.73 (d, 2 H, 10-CH_2), 5.83 (s, 2 H, 4-NH_2), 6.03 (t, 1 H, 9-NH), 7.06−7.14 (m, 3 H, 5,7,8-CH), 7.24 (s, 2 H, 2-NH_2), 7.44−7.60 (m, 4 H, Ar), 7.84 (d, 1 H, Ar), 7.94 (d, 1 H, Ar), 8.15 (d, 1H, Ar). Anal. calcd for ($C_{19}H_{17}N_5$·0.1H_2O·0.2CH_3COOH) C, H, N.

2,4-Diamino-6-[*N*-(2′,5′-dimethoxybenzyl)-*N*-methylamino]quinazoline, 11. Compound **11** was synthesized from **3** (0.10 g, 0.28 mmol), formaldehyde (0.04 g, l.l mmol), and sodium cyanoborohydride (0.05 g, 0.84 mmol) using procedure B to afford 0.09 g (81.4%) of **11** as a bright yellow solid: mp 143−144 °C; TLC R_f 0.57 ($CHCl_3$:CH_3OH:NH_4OH-5:2:0.5); ^{1}H NMR (DMSO-d_6) δ 2.93 (s, 3 H, N−CH_3), 3.55 (s, 3 H, OCH_3), 3.73 (s, 3 H, OCH_3), 4.46 (s, 2 H, 10-CH_2), 5.98 (s, 2 H, 4-NH_2), 6.48 (d, 1 H, Ar), 6.72 (q, 1 H, Ar), 6.88 (s, 2 H, Ar), 7.11 (s, 2 H, Ar), 7.15 (s, 1 H, Ar), 7.40 (s, 2 H, 2-NH_2). Anal. calcd for ($C_{18}H_{21}N_5O_2$·0.25H_2O·1.0 HCl) C, H, N.

2,4-Diamino-6-[*N*-(3′,4′-dimethoxybenzyl)-*N*-methylamino]quinazoline, 12. Compound **12** was synthesized from **4** (0.1 g, 0.28 mmol), formaldehyde (0.04 g, l.l mmol), and (0.05 g, 0.84 mmol) using procedure B to afford 0.09 g (86%) of **12** as a bright yellow solid: mp 230−231 °C; TLC R_f 0.61 ($CHCl_3$: CH_3OH:NH_4OH-5:2:0.5); ^{1}H NMR (DMSO-d_6) δ 3.26 (s, 3 H, N−CH_3), 3.64 (s, 6 H, 3′,5′-OCH_3), 4.47 (s, 2 H, 10-CH_2), 6.14 (s, 2 H, 4-NH_2), 6.32 (s, 3-H, Ar), 7.21 (m, 3 H, 5,7,8-CH), 7.55 (s, 2 H, 2-NH_2). Anal. calcd for ($C_{18}H_{21}N_5O_2$·0.2H_2O·0.2CH_3-COOH) C, H, N.

2,4-Diamino-6-[*N*-(2′,4′-dimethoxybenzyl)(methyl)amino]-quinazoline 13. Compound **13** was synthesized from **5** (0.1 g, 0.28 mmol), formaldehyde (0.04 g, l.l mmol), and (0.05 g, 0.84 mmol) using procedure B to afford 0.09 g (86%) of **13** as a yellow solid: mp 123−124 °C; TLC R_f 0.59 ($CHCl_3$:CH_3-OH:NH_4OH-5:2:0.5); ^{1}H NMR (DMSO-d_6) 2.91 (s, 3-H, NCH_3), 3.73−3.82 (m, 6 H, 2′,4′-OCH_3), 4.47 (s, 2 H, 10-CH_2), 6.40 (s, 2 H, 4-NH_2), 6.76 (m, 2 H, Ar), 7.06−7.23 (m, 4 H, Ar), 7.76 (s, 2 H, 2-NH_2). Anal. calcd for ($C_{18}H_{21}N_5O_2$·0.5H_2O·1.5 HCl) C, H, N.

2,4-Diamino-6-[*N*-(2′,3′,4′-trimethoxybenzyl)(methyl)-amino]quinazoline, 14. Compound **14** was synthesized from **7** (0.10 g 0.28 mmol), formaldehyde (0.04 g, l.l mmol), and (0.05 g, 0.84 mmol) using procedure B to afford 0.09 g (91%) of **14** as a yellow solid: mp 180−181 °C; TLC R_f 0.49 ($CHCl_3$:CH_3-OH:NH_4OH 5:2:0.5); ^{1}H NMR (DMSO-d_6) 2.91 (s, 3 H, N−CH_3), 3.73 (s, 6 H, OCH_3), 3.78 (s, 3 H, OCH_3), 4.47 (s, 2 H, 10-CH_2), 6.31 (s, 2 H, 4-NH_2), 6.70 (s, 2 H, Ar), 7.25 (m, 3 H, 5,7,8-CH), 7.70 (s, 2 H, 2-NH_2). Anal. calcd for ($C_{19}H_{23}N_5O_3$·0.2CH_3-$COOH$·0.3H_2O) C, H, N.

2,4-Diamino-6-[*N*-(2′,3′-naphthyl)(methyl)amino]quinazoline, 15. Compound **15** was synthesized from **10** (0.10 g, 0.28 mmol), formaldehyde (0.04 g, l.l mmol), and (0.05 g, 0.84 mmol) using procedure B to afford 0.09 g (87%) of **15** as a yellow solid: mp 262−263 °C; TLC R_f 0.47 ($CHCl_3$:CH_3OH: NH_4OH-5:2:0.5); ^{1}H NMR (DMSO-d_6) δ 3.06 (s, 3 H, N−CH_3), 5.09 (s, 2 H, 10-CH_2), 6.93 (s, 2 H, 4-NH_2), 7.14−8.09 (m, 10 H, Ar), 8.24 (s, 2 H, 2-NH_2). Anal. calcd for ($C_{20}H_{19}N_5$·0.5H_2O· 0.5HCl) C, H, N.

Structure Determination and Refinement. hDHFR was isolated and purified by Blakley as described[30] and crystals were grown by the hanging drop vapor diffusion method. The protein solution of hDHFR was incubated overnight at 4 °C with NADPH followed by the inhibitor, 1c. Protein droplets contained 62% ammonium sulfate in 0.1 M phosphate buffer, pH 7.0. Crystals grew in three weeks time and are rhombohedral, space group *R*3 with hexagonal indexing, and diffract to 2.1 Å resolution. The lattice constants for the ternary complex of hDHFR−NADPH−**1c** are 86.259 and 77.637 Å. Data were collected at room temperature on an Rigaku RaxisIIc area detector and the data processed with the Rigakau software. The Rmerge for 2σ data was 4.96% with a 3-fold redundancy. The overall completeness of the data was 86.4% and 63.6% for data in the shell between 2.0 and 2.1 Å The data for the ternary complex refined to 20.2% for data to 2.1 Å resolution are included in the Supporting Information.

The structure was solved by molecular replacement methods using the coordinates of hDHFR−NADPH−MTX.[22] Inspection of the resulting difference electron density map using the program CHAIN[31] running on a Silicon Graphics Elan Workstation revealed density for a ternary complex. The final cycles of refinement were carried out with the inhibitor **1c** and cofactor NADPH using the program PROLSQ.[32a,b] The Ramachandran conformational paramaters for the last cycle of refinement generated by PROCHECK[33] shows that 94.3% of the residues have the most favored conformation and none are in the disallowed regions.

Further refinement was continued for the ternary complex and the model was manually adjusted to fit its electron density values and verified by a series of OMIT maps calculated from the current model with deleted fragments. The highest thermal parameters (30−50 Å^2) of the protein residues are near the binding entrance and the flexible loop regions. The remaining side chain thermal parameters range from 10 to 25 Å^2. In the final stages of refinement, 102 water molecules were added in accord with the criteria of good electron density and acceptable hydrogen bonds to other atoms. The final refinement statistics are available in Supporting Information and available upon request. Coordinates have been deposited with the Protein Data Bank (1BOZ).

Acknowledgment. This work was supported in part by NIH Grants GM52811 (A.G.), GM40998 (A.G.), AI 41743 (A..G.), CA10914 (R.L.K.), and GM51670 (V.C.) and NIH Contracts NO1-AI-87240 (S.F.Q.) and NO1-AI-35171 (S.F.Q.), Division of AIDS. Human DHFR (F31G) was kindly provided by Dr. Raymond L. Blakley, St. Jude Children's Research Hospital, Memphis, TN 38101.

Supporting Information Available: Refinement statistics for the **1c**−NADPH−hDHRF complex (1 page). Ordering information is given on any current masthead page.

References

(1) Presented in part at the 211th American Chemical Society National Meeting, New Orleans, LA, March 24−28, 1996; Abstr: MEDI 182.

(2) Mills, J.; Masur, H. AIDS-Related Infections. *Sci. Am.* **1991**, August, 50−57.

(3) Klepser, M. E.; Klepser, T. B. Drug Treatment of HIV-related Opportunistic Infections. *Drugs* **1997**, *53* (1), 40−73.

(4) Levine, S. J. *Pneumocystis carinii. Clinics in Chest Med*. **1996**, *17* (4), 665−695.

(5) Allegra, C. J.; Kovacs, J. A.; Drake, J. C.; Swan, J. C.; Chabner, B. A.; Masur, H. Activity of Antifolates against *Pneumocystis carinii* Dihydrofolate Reductase and Identification of a Potent New Agent. *J. Exp. Med.* **1987**, *165*, 926−931.

(6) Masur, H.; Polis, M. A.; Tuazon, C. V.; Ogota, A. D.; Kovacs, J. A.; Katz, D.; Hilt, D.; Simmons, T.; Feuerstein, I.; Lundgren, B.; Lane, H. C.; Chabner, B. A.; Allegra, C. J. Salvage Trial of Trimetrexate-Leucovorin for the Treatment of Cerebral Toxoplasmosis. *J. Infect. Dis.* **1993**, *167*, 1422−1426.

(7) Kovacs, J. A.; Allegra, C. A.; Swan, J. C.; Drake, J. C.; Parillo, J. E.; Chabner, B. A.; Masur, H. Potent Antipneumocystis and Antitoxoplasma Activities of Piritrexim, a Lipid-soluble Antifolate. *Antimicrob. Agents Chemother*. **1988**, *32*, 430−433.

(8) Gordon, F. M.; Simin, G. L.; Wosby, C. B.; Mills, J. Adverse Reactions to Trimethoprim-Sulfamethoxazole in Patients with the Acquired Immunodeficiency Syndrome. *Ann. Intern. Med.* **1984**, *100*, 495−499.

(9) Gangjee, A.; Shi, J.; Queener, S. F.; Barrows, R. L.; Kisliuk, R. L. Synthesis of 5-Methyl-5-Deaza Nonclassical Antifolate as Inhibitors of Dihydrofolate Reductases and as Potential Anti-*Pneumocystis*, Anti-*Toxoplasma* and Antitumor Agents. *J. Med. Chem*. **1993**, *36*, 3437−3443.

(10) Gangjee, A.; Vasudevan, A.; Queener, S. F.; Kisliuk, R. L. 6-Substituted 2, 4-Diamino-5-Methyl-Pyrido[2,3-*d*]pyrimidines as Inhibitors of Dihydrofolate Reductases from *Pneumocystis carinii* and *Toxoplasma gondii* and as Antitumor Agents. *J. Med. Chem*. **1995**, *38*, 1778−1785.

(11) Gangjee, A.; Vasudevan, A.; Queener, S. F.; Kisliuk, R. L. 2,4-Diamino-5-Deaza-6-Substituted Pyrido[2,3-*d*]pyrimidines Antifolates as Potent and Selective Nonclassical Inhibitors of Dihydrofolate Reductases. *J. Med. Chem*. **1996**, *39*, 1438−1446.

(12) Gangjee, A.; Devraj, R.; McGuire, J. J.; Kisliuk, R. L.; Queener, S. F.; Barrows, L. R. Classical and Nonclassical Furo[2,3-*d*]-pyrimidines as Novel Antifolates: Synthesis and Biological Activities. *J. Med. Chem*. **1994**, *37*, 1169−1176.

(13) Gangjee, A.; Mavandadi, F.; Queener, S. F.; McGuire, J. J. Novel 2,4-Diamino-5-Substituted Pyrrolo[2,3-*d*]pyrimidines as Classical and Nonclassical Antifolate Inhibitors of Dihydrofolate Reductases. *J. Med. Chem*. **1995**, *38*, 2158−2165.

(14) Cody V.; Wojtczak, A.; Kalman, T. I.; Friesheim, J. H.; Blakley, R. L. Conformational Analysis Of Human Dihydrofolate Reductase Inhibitor Complexes: Crystal Structure Determination Of Wild-Type and F31 Mutant Binary and Ternary Inhibitor Complexes. *Adv. Exp. Med. Biol.* **1993**, *338*, 481−486.

(15) Champness, J. N.; Achari, A.; Ballantine, S. P.; Bryant, P. K.; Delves, C. J.; Stammers, D. K. The Structure of *Pneumocystis carinii* Dihydrofolate Reductase to 1.9 Å Resolution. *Structure* **1994**, *2*, 915−924.

(16) Piper, J. R.; McCaleb, G. S.; Montgomery, J. A.; Kisliuk, R. L.; Gaumont, Y.; Sirotnak, F. M. Synthesis and Antifolate Activity of 5-Methyl-5-Deaza-Analogues of Aminopterin, Methotrexate, Folic Acid and N-10 Methyl Folic Acid. *J. Med. Chem*. **1986**, *29*, 1080−1086.

(17) Hynes, J. B.; Harmon, S. J.; Floyd, G. G.; Farrington, M.; Hart, L. D.; Gale, G. R.; Washtein, W. L.; Susten, S. S.; Freisheim, J. H. Chemistry and Antitumor Evaluation of Selected Classical 2,4-Diaminoquinazoline Analogues of Folic Acid. *J. Med. Chem*. **1985**, *28*, 209−215.

(18) Schornagel, J. H.; Chang, P. K.; Sciarini, L. J.; Moroson, B. A.; Mini, E.; Cashmore, A. R.; Bertino, J. Synthesis and Evaluation of 2,4-Diamino Quinazoline Antifolates with Activity Against Methotrexate Resistant Human Tumor Cells. *Biochem. Pharmacol.* **1984**, *33*, 3251−3255.

(19) Tripos Associates, Inc., 1699 S. Hanely Road, Suite 303, St. Louis, MO 63144.

(20) Gangjee, A.; Vasudevan, A.; Queener, S. F. Synthesis and Biological Evaluation of Nonclassical 2,4-Diamino-5-methylpyrido[2,3-*d*]pyrimidines with Novel Side Chain Substituents as Potential Inhibitors of Dihydrofolate Reductases. *J. Med. Chem*. **1997**, *40*, 479−485.

(21) Cody, V.; Wojtczak, A.; Kalman, T. I.; Freisheim, J. H.; Blakley, R. L. Conformational Analysis of Human Dihydrofolate Reductase Inhibitor Complexes: Crystal Structure Determination of Wild-Type and F31 Mutant Binary and Ternary Inhibitor Complexes. *Adv. Exp. Biol. Med*. **1993**, 481−486.

(22) Cody, V.; Luft, J. R.; Ciszak, E.; Kalman, T. I.; Freisheim, J. H. Crystal Structure Determination at 2.3 Å of Recombinant Human Dihydrofolate Reductase Ternary Complex with NADPH and Methotrexate-γ-tetrazole. *Anti-Cancer Drug Des*. **1992**, *7*, 483−491.

(23) Blakley, R. L. Eukaryotic Dihydrofolate Reductase, *Adv. Enzymol.* **1995**, *70*, 23−102.

(24) Cody, V.; Galitsky, N.; Luft, J. R.; Pangborn, W.; Gangjee, A.; Devraj, R.; Queener, S. F.; Blakley, R. L. Comparison of the Ternary Complexes of *Pneumocystis carinii* and Wild-Type Human Dihydrofolate Reductase with a Novel Classical Antitumor Furo[2,3-*d*]pyrimidine Antifolate. *Acta Cryst.* (*D*) **1997**, *D53*, 638−649.

(25) Broughton, M. C.; Queener S. F. *Pneumocystis carinii* Dihydrofolate Reductase Used to Screen Potential Antipneumocystis Drugs. *Antimicrob. Agents Chemother.* **1991**, *35*, 1348−1355.

(26) Chio, L.; Queener, S. F. Identification of Highly Potent and Selective Inhibitors of *Toxoplasma gondii* Dihydrofolate Reductase. *Antimicrob. Agents Chemother.* **1993**, *37*, 1914−1923.

(27) Piper, J. R.; Johnson, C. A.; Maddry, J. A.; Malik, D. N.; McGuire, J. J.; Otter, G. M.; Sirotnak, F. M. Studies on Analogues of Classical Antifolates Bearing the Naphthoyl Group in Place of the Benzoyl in the Side Chain. *J. Med. Chem*. **1993**, *36*, 4161−4171.

(28) Kisliuk, R. L.; Strumpf, D.; Gaumont, Y.; Leary, R. P.; Plante, L. Diastereisomers of 5,10-Methylene-5,6,7,8-Tetrahydropteroyl-D-Glutamic Acid. *J. Med. Chem*. **1977**, *20*, 1531−1533.

(29) We thank the Developmental Therapeutics Program of the National Cancer Institute for performing the in vitro anticancer evaluation.

(30) Chunduru, S. K.; Cody, V.; Luft, J. R.; Pangborn, W.; Appleman, J. R.; Blakley, R. L. Methotrexate-resistant Variants of Human Dihydrofolate Reductase: Effects of Phe31 Substitutitons. *J. Biol. Chem*. **1994**, *269*, 9547−9555.

(31) Sack, J. S. CHAIN − A Crystallographic Modeling Program. *J. Mol. Graphics* **1988**, *6*, 224−225.

(32) (a) Hendrickson, W. A.; Konnert, J. H. In *Computing in Crystallography*; Diamond, R., Rameshan, S., Venkatesan, K., Eds.; Indian Academy of Sciences: Bangalore, India, 1980; p 13.0. (b) Finzel, B. C. Incorporation of Fast Fourier Transform to Speed Restrained Least-Squares Refinement of Protein Structures. *J. Appl. Crystallogr*. **1987**, *20*, 53−57.

(33) Laskowski, R. A.; MacArthur, M. W.; Doss, D. S.; Thornton, J. M. PROCHECK: A Program to Check the Stereochemical Quality of Protein Structures. *J. Appl. Crystallogr*. **1993**, *26*, 2891.

JM980081Y